Metal-Organic Frameworks as Hosts for Fluorinated Azobenzenes: A Path towards Quantitative Photoswitching with Visible Light

Daniela Hermann, Heidi Schwartz, Melanie Werker, Dominik Schaniel, Uwe Ruschewitz

Metal-Organic Frameworks as Hosts for Fluorinated Azobenzenes: A Path Towards Quantitative Photoswitching

Daniela Hermann,[†] Heidi A. Schwartz,[†] Melanie Werker,[†] Dominik Schaniel,[§] Uwe Ruschewitz*,[†]

[†]University of Cologne, Department of Chemistry, Greinstraße 6, D-50939 Cologne, Germany

[§]Université de Lorraine, CNRS, CRM², F-54506 Nancy, France

KEYWORDS. Azobenzene, fluorinated derivatives, metal-organic framework, photochromism, solid state switching

ABSTRACT: Fifteen new photochromic materials were synthesized by gas phase loading of fluorinated azobenzenes, namely *ortho*-tetrafluoroazobenzene (*tF*-AZB), 4H,4H'-octafluoroazobenzene (*oF*-AZB), and perfluoroazobenzene (*pF*-AZB), into the pores of the well-known metal-organic frameworks MOF-5, MIL-53(Al), MIL-53(Ga), MIL-68(Ga), and MIL-68(In). Their composition was analyzed by elemental (CHNS) and DSC/TGA analysis. For *pF*-$AZB_{0.34}$@MIL-53(Al) a structural model based on high-resolution synchrotron powder diffraction data was developed and the host-guest and guest-guest interactions were elucidated from this model. These interactions of O-H···F and π···π type were confirmed by significant shifts of the O-H frequencies in loaded and unloaded MOFs of the MIL-53 and MIL-68 series. Most remarkably, some of the synthesized *F*-AZB@MOF systems show almost quantitative (> 95 %) switching between its *E* and *Z* isomers and no significant fatigue after repeated switching cycles.

INTRODUCTION

Photochromic materials have found wide-spread applications e.g. in colour changing sunglasses[1] or as data storage devices.[2] According to *Hirshberg* photochromism is the reversible structural transformation of a molecular entity between two configurations induced by irradiation with electromagnetic waves leading to a change of the resulting absorption properties.[3] These structural changes are for example *E*/*Z* isomerizations (e.g. azobenzenes, stilbenes) or ring-opening/-closing reactions (e.g. spiropyrans, diarylethenes).[1] For all of them the structural transformation typically leads to significant changes of the size, shape and properties like dipole moments of these molecules so that their photochromic behaviour is largely influenced by the surrounding medium. Thus the photoswitching behaviour is well established in solution,[4-8] but mainly suppressed in crystalline solids of the respective molecules due to spatial hindrance. Accordingly, for potential applications the photochromic molecular entities are incorporated in polymers[9-11], crystalline[12] and amorphous thin films[13-15], porous matrices like zeolites[16-18], or molecular cages.[19-20]

Recently, metal-organic frameworks (MOFs) were established as a new class of host materials for photochromic guests.[21-23] MOFs are hybrid materials consisting of inorganic knots, chains or layers (mainly metal-oxo units), which are bridged by rigid multifunctional organic molecules or anions (named "linker") to form crystalline porous materials with a very high structural flexibility.[24,25] To incorporate the photochromic functionality into these MOFs three general approaches were described:

1) The photochromic entity is part of the linker backbone of the respective MOF.[26-27] But it is a severe drawback of this approach that the large structural changes upon irradiation often lead to a degradation of the framework.
2) The photochromic functionality is added as a substituent to the linker.[28-37] This leads to the necessary sterical freedom for successful photoisomerisation, but like for 1) typically elaborate synthetic efforts are needed to obtain these linker molecules.
3) The most simple way is to directly embed the photochromic molecules into the empty pores of a MOF by gas phase loading or by solution based processes.[38] Not only the low synthetic efforts, but also the high flexibility with respect to the embedded guests are advantages of this approach.

In the following we will focus on approach 3), which has successfully been used to embed azobenzene dyes,[39,40] spiropyrans/merocyanines[41,42] and diarylethenes[43-45] in different MOF hosts. For all of them successful photoswitching of the embedded guests was proven.

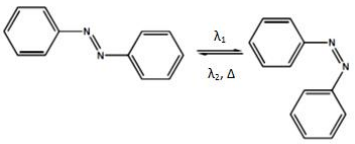

Scheme 1. *E*/*Z* isomerization of azobenzene (AZB).

The *E*/*Z* isomerisation of azobenzene (abbreviated to AZB in the following), which is shown in Scheme 1, can be regarded as the prototype of photochromism. The successful embedment of AZB into the MOFs MOF-5,[40] MIL-68(In),[40] MIL-68(Ga),[40] MIL-53(Al),[40] and DMOF-1[39] was already shown, and for the latter the remote-controlled uptake and release of CO_2 was proven.[39] It is however a severe drawback of AZB that UV light that might interfere with the host matrix, is needed to induce the *E*/*Z* isomerisation. Even more, the overlapping absorption bands of the *E* and *Z* isomers lead to photostationary states, i.e. a complete photoswitching of pristine AZB from *E* to *Z* and vice versa is not possible. For example, in zeolite NaY > 90 % *Z*-AZB were achieved, but here the formation of a Na^+-AZB complex was postulated.[46] For $AZB_{0.66}$@MIL-68(In) we reached a maximum of ca. 30 % of the excited *Z* state under illumination with UV light (λ = 325 nm),[40] whereas Yanai et al. found 38 % of the *Z* isomer in AZB@DMOF-1 after UV light irradiation using an ultra-high-pressure Hg lamp.[39] However, it was shown that modifying AZB with suitable substituents will separate the absorption bands of the *E* and *Z* isomers to overcome these limitations.[47] A very elegant way is the introduction of fluorine atoms in the phenyl rings of AZB. For *ortho*-tetrafluoroazobenzene (*tF*-AZB) photostationary states with 91 % *Z* and 86 % *E* states were reached in acetonitrile solutions.[48] Furthermore the wavelengths needed to trigger the photo-isomerization are shifted to the visible region of the spectrum so that no longer UV light has to be applied. It was successfully shown that incorporating *tF*-AZO side groups attached to suitable linker molecules into MOF structures leads to solid materials with almost quantitative *E*/*Z* isomerization, which can be switched with green and violet light, respectively.[35,36] In the following we will show that also by direct embedment of fluorinated derivatives of AZB in different MOF hosts following approach 3) (s. above) photochromic guest@MOF systems with an almost quantitative *E*/*Z* photoswitching with visible light can be obtained. Furthermore we examined the underlying host-guest interactions occurring in these guest@MOF systems and show how they influence the photoswitching properties of these composite materials. The fluorinated AZB derivatives used in this work are given in Scheme 2. Some of their optical properties are summarized in Table 1. The superior photoswitching properties of *tF*-AZB are obvious from this compilation. For thin (SURMOF) films of type HKUST-1 the successful incorporation of *tF*-AZB was already proven.[49] The crystal structures of *E*- and *Z*-*tF*-AZB were reported quite recently and compared with those of the other azobenzenes depicted in Scheme 2.[50]

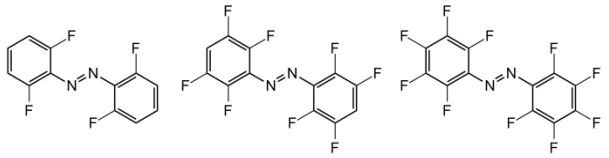

Scheme 2. *E* isomers of *ortho*-tetrafluoroazobenzene (*tF*-AZB), 4H,4H'-octafluoroazobenzene (*oF*-AZB), and perfluoroazobenzene (*pF*-AZB) (f.l.t.r.).

<Table 1>

EXPERIMENTAL SECTION

MOF synthesis. The colourless and well-established metal-organic frameworks MOF-5,[53] MIL-53(Al),[54] MIL-53(Ga),[55] MIL-68(Ga),[56] and MIL-68(In)[56] were selected for this investigation. Details of their syntheses are given in the Supporting Information. MOF-5 was provided by BASF and used without any further purification.

Synthesis of fluorinated azobenzenes. For the synthesis of ***tF*-AZB** and ***oF*-AZB** we used the protocol that was described earlier in detail.[50] *tF*-AZB: $C_{12}H_6F_4N_2$ (254.19): Calcd – C, 56.70%, H, 2.38%, N, 11.02%; Found – C, 56.92%, H, 2.89%, N, 10.35%; *oF*-AZB: $C_{12}H_2F_8N_2$ (326.15): Calcd – C, 44.19%, H, 0.62%, N, 8.59%; Found – C, 44.64%, H, 0.85%, N, 7.96%.

***pF*-AZB** was synthesized mainly following the procedures given in the literature.[57,58] 500,0 mg pentafluoroaniline (2.73 mmol) were dissolved in 30 mL toluene and 3.03 g Lead(IV)-acetate (6.83 mmol) were added, whereon the suspension turned red. After stirring at room temperature overnight the brown precipitate was filtered off. The solution was washed with acetic acid (50%) and the organic phase was dried with $MgSO_4$. After removing the solvent at reduced pressure the residue was purified by column chromatography (CH_2Cl_2 : *cyclo*-hexane 3 : 7). 128.8 mg (yield: 37%) perfluoroazobenzene were obtained as a red solid. NMR signals were assigned according to the literature:[58] ^{19}F-NMR (282MHz, $CDCl_3$): δ /ppm=-161.2 (m, 4F, trans-2F, 2'F, 6F, 6'F), -158,6 (m, 4F, cis-2F, 2'F, 6F, 6'F), -150,4 (m, 2F, cis-4F, 4'F), -148,3 (m, 6F, trans-F3, F3', F4, F4', F5, F5'), -146,6 (m, 4F, cis-F3, F3', F5, F5'). $C_{12}F_{10}N_2$ (362.13): Calcd – C, 39.80%, H, 0%, N, 7.74%; Found – C, 39.65%, H, 0.40%, N, 6.77%. Small amounts of hydrogen might result from minor amounts of moisture or solvents (CH_2Cl_2 or *cyclo*-hexane).

Preparation of guest@MOF systems (guest: *tF*-AZB, *oF*-AZB, *pF*-AZB). In general a mixture of the respective activated MOF was loaded with the azobenzene via a gas phase procedure. Under reduced pressure (~5×10^{-2} mbar) the respective AZB guest was sublimed on to the activated MOF, which was heated from 50 °C to 70 °C (*tF*-AZB) or 75 °C (*oF*-AZB, *pF*-AZB) for 2-3 hours. The end of the loading process was recognized, when no longer red crystals of the azobenzene are visible on the MOF material. The excess of the respective azobenzene resublimated at the top of the glass tube. To prevent the absorption of water or the de-

composition of the MOF upon contact with air and moisture, all compounds were stored in a glovebox under a dry argon atmosphere (H_2O < 1 ppm, O_2 < 1 ppm), where all further handling was carried out. In Table S1 (Supporting Information) the detailed weighted samples of all experiments are listed. A photograph of some of the resulting powders is given as Figure S5 (Supporting Information). The purity and composition of the resulting composites guest@MOF were analyzed by XRPD (Le Bails fits: Table S2, Figures S6-S19 in the Supporting Information) and elemental analysis (Table S3, Supporting Information). The resulting compositions are summarized in Tables S4 (Supporting Information). Details of the methods are given below and the results are discussed in the next paragraph.

X-ray Powder Diffraction. Laboratory measurements were carried out on a STOE Stadi P diffractometer (Ge monochromator, PSD detector) with Cu $K\alpha_1$ radiation. Data were collected at 298 K between 4 and 80.59° in 2θ with steps of 0.01° and a measurement time of 5 s/step. For each sample four such scans were added. Alternatively, data were recorded on a Huber G670 diffractometer (Ge monochromator, image plate detector, room temperature, Cu $K\alpha_1$ radiation), ca. 120-800 min per scan. Samples were sealed in glass capillaries (∅ = 0.3 – 0.5 mm) under inert conditions (Argon filled glovebox) prior to all measurements.

Synchrotron Powder Diffraction. High-resolution synchrotron powder diffraction data were recorded at the Swiss Norwegian BeamLine (SNBL, BM01B)[59] at the European Synchrotron (ESRF, Grenoble/France). The wavelength was calibrated with a Si standard NIST 640c to 0.50195 Å and 0.50544 Å, respectively. The diffractometer is equipped with six counting channels, delivering six complete patterns collected with a small 1.1° offset in 2θ. A Si(111) analyzer crystal is mounted in front of each NaI scintillator/photomultiplier detector. Data were collected at 298 K and 120 K (cryostreamer) with steps of 0.002° (2θ) and 100-500 ms of integration time per data point. Typical recording times were 20-60 min per scan. For each sample 5-8 such scans were added. Data from all detectors and scans were averaged and added to one pattern with local software.

An additional synchrotron powder diffraction pattern was collected at beamline BL9 of the DELTA synchrotron radiation facility, Dortmund.[60] The measurement was performed at 295 K with a wavelength of λ = 0.81577 Å using a NaI scintillation detector.

For all experiments the substances were filled in glass capillaries (∅ = 0.7 – 1.0 mm) and sealed under an argon atmosphere. The capillaries were mounted on spinning goniometers.

Analysis of powder diffraction data. The WinXPow software package[61] was used for raw data handling and visual inspection of the data. To determine the unit cell parameters of the resulting guest@MOF systems precisely, Le Bail fits in Jana2006[62] were performed by refining the lattice parameters, zero shift, background, and profile parameters (pseudo-Voigt) for each pattern. Depending on the instrument also parameters for reflection asymmetry and anisotropy were included in the refinements. The results of these Le Bails fits are summarized in Table S2 and the plots of these fits are shown in Figures S6-S19 (all Supporting Information). They were visualized using Gnuplot 4.6.[63]

Structure Solution and Refinement. The high quality diffraction pattern of *pF*-$AZB_{0.34}$@MIL-53(Al) obtained at the ESRF at 120 K was used to elucidate the arrangement of the guest within the pores of this MOF. For the structure solution, the atomic positions of MIL-53(Al)·0.7H_2bdc[64] were used as starting parameters of the host together with the unit cell parameters obtained from the Le Bail fits. Furthermore, the known molecular structure of *E*-perfluoroazobenzene[65] was introduced on the starting position 0 0 0 in FOX.[66] The global optimization algorithm was run in the parallel tempering mode and converged after approximately 130000 trials for *pF*-AZB@MIL-53(Al) (R_p = 0.2452 and wR_p = 0.1699). The occupancy of *pF*-AZB was fixed at 0.125 in the solution process. The resulting structural model was used as a starting model for a Rietveld refinement with GSAS.[67] To get a stable refinement, the *E*-perfluoroazobenzene molecules, as well as the benzenedicarboxylate anions of the MOF, were fixed with soft constraints (bond lengths, angles, and planes according to the literature values).[64,65] The isotropic displacement parameters of the atoms of the *pF*-AZB guest and the host were coupled with constraints and refined afterward, if possible. In the final refinements also the occupancy of the guest was refined resulting in *pF*-$AZB_{0.34}$@MIL-53(Al). This occupancy is in good agreement with the result of the elemental analysis: *pF*-$AZB_{0.3}$@MIL-53(Al) (Tables S3 and S4, Supporting Information). The final refinement of *pF*-$AZB_{0.34}$@MIL-53(Al) converged slowly with a total of 119 parameters (R_p = 0.0858 and wR_p = 0.1082). The resulting fit is given as Figure S20 and selected details of the Rietveld refinement are summarized in Table S5, both Supporting Information. The reliability of the resulting structural model is corroborated by the good fit (Figure S20), the almost coincident agreement of the occupancy factors obtained from Rietveld refinement (0.34) and elemental analysis (0.30) as well as the reasonable resulting distances between the *pF*-AZB guest and the MOF host, which will be discussed later. Diamond[68] was used for the visualization of the crystal structure of *pF*-$AZB_{0.34}$@MIL-53(Al).

Elemental Analysis. Elemental analysis of carbon, hydrogen, and nitrogen was performed with a HEKAtech GmbH EuroEA 3000 Analyzer. In a glovebox, approximately 2 mg of each compound was filled into a tin cartridge. Theoretical values were calculated for different ratios guest:host and compared with the experimental values. The composition with the best agreement in all three values (C, H, N content) was chosen as the most likely one and used in the following (Tables S3 and S4 in the Supporting Information). Compounds with MIL-53(Ga) as host were excluded from these calculations, as weak extra reflections in the XRPD patterns of the as-synthesized MOF indicated that it was not obtained as a single-phase product.

NMR spectroscopy. ^{1}H and ^{19}F NMR spectra were recorded on a BRUKER Avance 300 MHz spectrometer in deuterated $CDCl_3$ solutions at room temperature (^{1}H: 300.13 MHz; ^{19}F: 282 MHz). The spectra were analyzed with the ACD/NMR Processor software.[69]

IR spectroscopy. IR spectra without illumination were recorded with a Bruker ALPHA FT-IR spectrometer (Platinum ATR module and diamond crystal). The spectrometer was housed in a glovebox (Argon atmosphere) to provide inert conditions. IR measurements under photo-irradiation were performed on transparent KBr pellets (dried at 60 °C; 10 t for 30 min) on a Nicolet 5700 spectrometer (250 – 4000 cm^{-1}, resolution: 2 cm^{-1}). During the measurements the sample chamber was evacuated to 10^{-5} bar to enhance the quality of the spectra as well as to improve the life time of the transparent pellets. After recording the IR spectra of the ground state, the compounds were illuminated with 532 nm laser light to induce the $E \rightarrow Z$ isomerization. To investigate the reconversion to *E*-azobenzenes, the compounds were illuminated with 405 nm laser light. For *tF*-AZB also illumination with λ = 476 nm was tested (Figure 6). The following exposure times (t_{exp}) and radiant exposures (E/A) were applied for the different fluorinated AZB guests: *pF*-AZB (t_{exp} = 30-60 min; E/A = 24-95 J/cm²), *oF*-AZB (t_{exp} = 15-58 min; E/A = 12-95 J/cm²), and *tF*-AZB (t_{exp} = 23-126 min; E/A = 23-278 J/cm²). For *pF*-AZB (t_{exp} = 780 min) and *tF*-AZB (t_{exp} = 840 min) also long exposures overnight were tested.

For a quantitative analysis the extinctions of the bands of the *E* and *Z* isomers were determined (integration of the areas under the respective IR peaks after subtraction of the base line) and the maximum amount of the respective isomer was calculated based on the linear relationship between the concentration of a species and the extinction in the measured IR spectrum (Lambert-Beer law). In those systems, where a complete isomerization of one isomer was observed after irradiation, the amount of this isomer in the other spectra was directly calculated by relating it to this 100 % value. However, in most of the investigated systems no complete isomerization was obtained so that the extinction for 100% *E* or *Z* isomer had to be calculated using the following procedure: for each isomer one characteristic band with a strong intensity change after irradiation was chosen. From the change of the peak intensities for the highest and lowest amount of both isomers and the remaining intensities that were not extinguished by irradiation completely, the theoretical extinctions for 100 % *E* and 100 % *Z* isomer were estimated. Whenever possible, several such peaks were examined and a mean value was calculated. These mean values were used to determine the relative amounts of both isomers. A worked example is given on page 3 of the Supporting information to illustrate this procedure

DSC/TGA. DSC/TGA measurements were performed with a *Mettler Toledo* TGA/DSC 1 Star^{e} (Al_2O_3 crucible; Ar stream with 30 mL/min; heating rate 10 °C/min). Samples of approx. 2 - 6 mg were weighed out and handled under inert conditions (glovebox). Diagrams are visualized with Origin 8.5.0.[70]

RESULTS AND DISCUSSION

Synthesis, Composition & Stability

A few years ago we started to establish MOFs as suitable hosts for the embedment of photochromic guests like azobenzenes[40] and spiropyrans[42]. To embed the photochromic guests we developed a gas phase synthesis (see Experimental Section).[40,42] Gas phase loading and loading of the molten guest[39,43] are preferable to solution based processes, as with the former any solvents may be excluded from all further considerations. Using this gas phase approach we obtained highly crystalline materials, which were easily characterized by XRPD (X-ray powder diffraction) methods. In Figure 1 the XRPD patterns of activated ("empty") MIL-68(Ga) and loaded with different photochromic azobenzene guests (pristine azobenzene, *tF*-AZB, *oF*-AZB, *pF*-AZB) are shown. As the 2θ values of the reflections are mainly unchanged after loading, it can be concluded that the MOF framework is still intact. But as the reflection intensities are drastically modulated depending on the scattering power of the embedded guest, i.e. with increasing fluorine substitution, XRPD can be used as a simple and fast method to confirm the successful embedment of the guest. If the guest is not completely embedded in the MOF, additional reflections of the respective guest are visible in the XRPD pattern (not shown). Then these residues of the guest have to be removed by further heating in vacuum. Even more, for spiropyran, which was attempted to be embedded in MIL-53(Al), we showed that unchanged intensities after potential gas phase loading are a clear indicator that (almost) no embedment of the guest within the pores of the MOF has taken place.[42] In Figure S21 (Supporting Information) XRPD patterns of MOF-5 loaded with different starting ratios of pristine azobenzene are shown. These patterns show that a rough estimate of the quantitative amount of the embedded guest can be obtained.

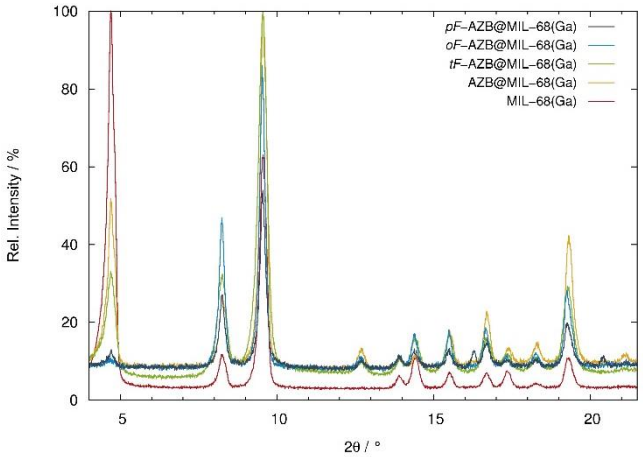

Figure 1. Sections of the XRPD patterns of MIL-68(Ga)*ht* (red), AZB@MIL-68(Ga) (yellow), *tF*-AZB@MIL-68(Ga) (green), *oF*-AZB@MIL-68(Ga) (turquois), and *pF*-AZB@MIL-68(Ga) (gray) (STOE Stadi P; capillaries, $CuK\alpha_1$ radiation).

Compared with attempts to incorporate the photoactive functionality as a part of the backbone or a substituent of the linker used to construct the respective MOF the approach to embed the photochromic molecule as a guest in the MOF framework has the advantage of an easy synthetic accessibility as well as a very high versatility with respect to the MOF and the guest. One might object that the guest molecules are only weakly bonded to the MOF framework so that the thermal stability of the resulting guest@MOF systems is not high, but for azobenzene embedded in thin films of type HKUST-1 it was shown that when stored at room temperature the guest leaves the MOF very slowly with a depletion (or desorption) time constant $\tau \approx 360$ days.[49] However, when stored at 60 °C τ decreases significantly to 14.5 days.[49] For two *pF*-AZB containing systems of this investigation the resulting DSC/TGA curves are shown in Figure 2 and Figure S22 (Supporting Information). They show that *pF*-AZB is released from MIL-53(Al) above approx. 150 °C (Figure 2), whereas from MOF-5 the release already starts at 100 °C (Figure S22). So the influence of the respective MOF host on the thermal stability of the resulting guest@MOF system is obvious. Nonetheless, both systems are stable at room temperature and the loss of *pF*-AZB at this temperature can be neglected. From the TGA curve of *pF*-$AZB_{0.34}$@MIL-53(Al) (Figure 2) a mass loss of 34.6 % is obtained leading to the composition *pF*-$AZB_{0.30}$@MIL-53(Al), which is in very good agreement with the results of the Rietveld and elemental analysis (Table S4, Supporting Information). The smooth DSC curve confirms that neither a decomposition of the guest or the host occurs up to 500 °C. The decomposition of the MOF starts above 500 °C (not shown), which is in good agreement with its decomposition temperature given in the literature ($T_{dec.}$ = 500 °C).[54] A small peak in the TGA curve at ca. 250 °C (Figure 2) is an artefact of the balance in this measurement.

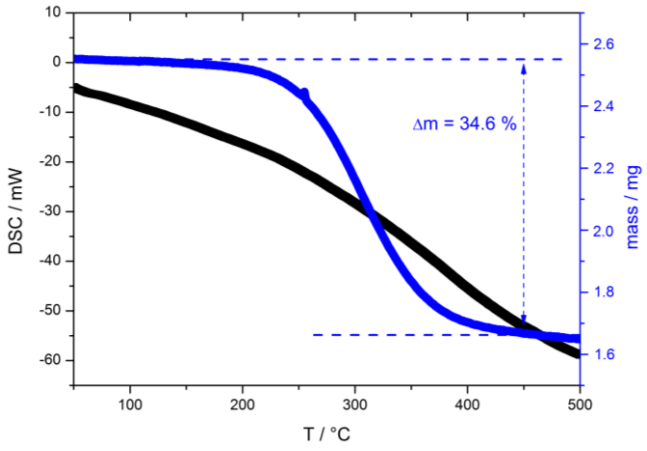

Figure 2. DSC/TGA curve of *pF*-$AZB_{0.34}$@MIL-53(Al).

Similar results were obtained for *pF*-AZB embedded in MOF-5 (Figure S22, Supporting Information). The mass loss of 61.5 % leads to the composition *pF*-$AZB_{3.40}$@MOF-5, which is again in very good agreement with the results of the elemental analysis: *pF*-$AZB_{3.57}$@MOF-5 (Table S4, Supporting Information). Here, the decomposition of the MOF framework already starts at 400 °C, as known for MOF-5.[53]

Crystal Structure & Host-Guest Interactions

To clarify the arrangement of the fluorinated azobenzene guest embedded in a MOF host and to understand the underlying host-guest interactions as well as to confirm the reliability of the compositions obtained from elemental and DSC/TGA analysis we performed a comprehensive structural analysis with a subsequent Rietveld refinement on a selected compound. For this analysis we have chosen *pF*-AZB embedded in MIL-53(Al) for the following reasons: according to Table 3 the ground state of *pF*-AZB consists to 100 % of the *E* isomer, so that in the refinements only this isomer has to be taken into account. Furthermore, the host MIL-53(Al) shows orthorhombic symmetry, which minimizes possible disorder compared to a MOF with a higher, i.e. cubic symmetry like MOF-5. It should be noted that compared to already published $AZB_{0.50}$@MIL-53(Al) (*P*nma, no. 62)[40] a symmetry change occurred for *pF*-AZB_x@MIL-53(Al) (*I*mma, no. 74). Details of the structure solution and refinement are given in the Experimental Section, in Figure 3 views of the resulting crystal structure are given. A space-filling representation was chosen to show that the guest molecules fit nicely into the pores of MIL-53(Al) taking the respective van der Waals radii into account. H···F distances between the BDC^{2-} linkers of the MOF and *pF*-AZB guests start at 295 pm. This value is as expected larger than the sum of the van der Waals radii of H and F (256 pm).[71] The position of the *pF*-AZB molecule is only occupied with an occupancy factor of less than 10 % resulting in the composition *pF*-$AZB_{0.34}$@MIL-53(Al). This value, which will be used in the following to name this compound, is in reasonable agreement with the results of the elemental (*pF*-$AZB_{0.27}$@MIL-53(Al)) and DSC/TGA analysis (*pF*-$AZB_{0.30}$@MIL-53(Al), Table S4, Supporting Information).

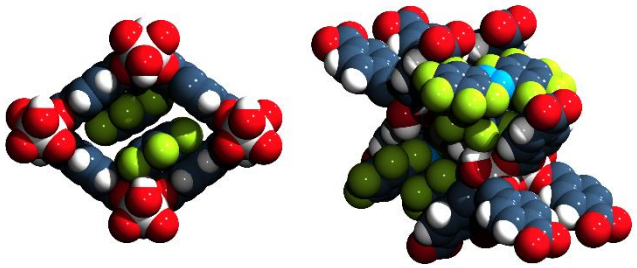

Figure 3. Space-filling presentation of the crystal structure of *pF*-$AZB_{0.34}$@MIL-53(Al) with a view along a channel ([100] direction, left) and a side-view with an "opened" channel (right); Al: large white, C: grey, O: red, H: small white, F: green, N: blue spheres.

In our former work on pristine azobenzene (AZB) embedded in different MOFs we presented the crystal structures of $AZB_{0.50}$@MIL-53(Al) and $AZB_{0.66}$@MIL-68(Ga).[40] As in all these investigations (Rietveld, elemental and DSC/TGA

analysis) a good agreement for the amount of the embedded guest molecules was found, we conclude that all methods are suitable to quantify the loading. In Figure 4 the dominating host-guest interactions in $AZB_{0.50}$@MIL-53(Al)[40] and *pF*-$AZB_{0.34}$@MIL-53(Al) are compared, as assigned after close inspection of both crystal structures. In $AZB_{0.50}$@MIL-53(Al) O-H···π interactions between the hydroxyl group of the MOF and both phenyl rings of AZB (O-H···C = 265 and 276 pm) are found. These interactions are depicted in Figure 4 (left) as dashed lines. Furthermore a parallel orientation of the phenyl rings of the BDC^{2-} linkers and the AZB guests suggests π···π interactions. The planes of two AZB guests are separated by 349 pm and the planes of a guest and a BDC^{2-} linker by 382 pm. So for the latter only weak interactions must be assumed, although in both cases the ring systems are shifted by approx. 300 pm pointing to a parallel displaced stacking (offset stacked). Some host-guest interactions found in *pF*-$AZB_{0.34}$@MIL-53(Al) are depicted in Figure 4 (right). Contrary to $AZB_{0.5}$@MIL-53(Al) O-H···F interactions (shortest O-H···F distance: 213 pm) seem to dominate and no O-H···π interactions are observed (shortest O-H···C distance: 281 pm compared to 265 pm in $AZB_{0.50}$@MIL-53(Al)). But this finding is not surprising, as the high degree of fluorination of the *pF*-AZB guest leads to an inversion of its quadrupole moment, i.e. the fluorine substituents bear the negative charge and the aromatic ring can no longer act as an electron donor.[72] The shortest C-C distance between two guest molecules is 322 pm, but the orientation of the phenyl rings is not in agreement with attractive π···π interactions. Such orientation is found at a C-C distance of 344 pm compared to 334 pm in $AZB_{0.5}$@MIL-53(Al). 320 pm is found as the shortest C-C distance between a *pF*-AZB guest and the BDC^{2-} linker. The rings are arranged almost directly one above each other with only a very small shift (between a stacked and an offset stacked arrangement).[73] Again this can be explained by the inverted quadrupole moment of the perfluorinated ring, which interacts with the unfluorinated phenyl ring of the BDC^{2-} linker. These interactions lead to a slight shift of $\tilde{\nu}$(C=C) from 1506 cm^{-1} in the IR spectrum of unloaded MIL-53(Al) to 1513 cm^{-1} in the IR spectrum of *pF*-$AZB_{0.34}$@MIL-53(Al). All these structural interpretations of interactions are complicated by the fact that the positions of the guest molecules are only partly occupied in $AZB_{0.50}$@MIL-53(Al) (occ. = 0.25) and *pF*-$AZB_{0.34}$@MIL-53(Al) (occ. = 0.086).

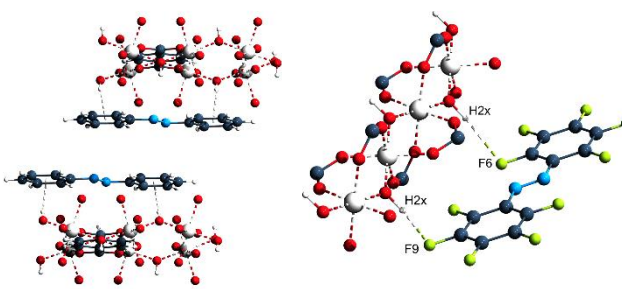

Figure 4. Details of the crystal structures of $AZB_{0.5}$@MIL-53(Al)[40] (left) and *pF*-$AZB_{0.34}$@MIL-53(Al)[this work] (right) emphasizing some of the occurring host-guest interactions; color coding as in Figure 3.

To analyze these host-guest and guest-guest interactions in more detail IR spectra of the activated ("empty") and loaded MOF were recorded. Especially the MOFs of type MIL-53 and MIL-68 are well-suited for such investigations, as the OH groups in these MOFs are very sensitive probes for such interactions. All samples were prepared under inert conditions (glovebox) and the spectrometer itself was also housed in a glovebox to provide completely inert conditions and to exclude any water impurities. In Table 2 the shifts of the resulting O-H frequencies are summarized as $\Delta\tilde{\nu}$ values, i.e. referenced to $\tilde{\nu}$(OH) of the activated ("empty") MOF.

Table 2. Shifts of IR frequencies of O-H stretching vibrations in loaded MOFs of the MIL-53 and MIL-68 series referenced to the activated MOF.

	E isomer $\Delta\tilde{\nu}$ / cm^{-1}	*Z* isomer $\Delta\tilde{\nu}$ / cm^{-1}
$AZB_{0.50}$@MIL-53(Al)	-39	-39
tF-$AZB_{0.19}$@MIL-53(Al)	-11 / -17*	-28
pF-$AZB_{0.34}$@MIL-53(Al)	-10	-10
$AZB_{0.66}$@MIL-68(Ga)	-39	-39
tF-$AZB_{0.58}$@MIL-68(Ga)	-14	-24
pF-$AZB_{0.63}$@MIL-68(Ga)	-3 / -10*	-3 / -10*
$AZB_{0.66}$@MIL-68(In)	-55	-55
tF-$AZB_{0.57}$@MIL-68(In)	-49	-12
pF-$AZB_{0.32}$@MIL-68(In)	-16	-16

* split signals

The most significant shifts were obtained for AZB as guest. This points to the fact that the O-H···π and π···π interactions discussed for $AZB_{0.50}$@MIL-53(Al) are obviously stronger than the O-H···F and π···π interactions found in *pF*-$AZB_{0.34}$@MIL-53(Al). The guest-guest and host-guest interactions with *tF*-AZB seem to be somewhere in-between: in MIL-68(In) a strong shift was found, whereas smaller shifts are observed for *tF*-AZB embedded in MIL-53(Al) and MIL-68(Ga). One might speculate that *tF*-AZB is able to form different types of interactions (O-H···F, C-H···π etc.), which are dependent on the specific arrangement of the guest within the MOF pores. This is supported by the significant shifts upon $E \rightarrow Z$ isomerization, which are specific for *tF*-AZB as guest. This will be discussed in more detail in the next chapter, where also a correlation between the photochromic properties and the host-guest and guest-guest interactions, as indicated by the results documented in Table 2, will be attempted.

Photochromic Properties

In our previous work we showed that IR spectroscopy is well-suited to characterize the photochromic behavior of azobenzene[40] and spiropyran[42] embedded in different MOF hosts due to the fact that the IR bands of the guest hardly overlap with those of the MOF host (Figure 5). Therefore it allows for a direct quantitative analysis of the switching process via the determination of the changes in the area of the relevant IR bands. This procedure seems to be preferable to the elution of the guest and analysis of the *E*/*Z* ratio by e.g. ultraperformance liquid chromatography (UPLC).[52]

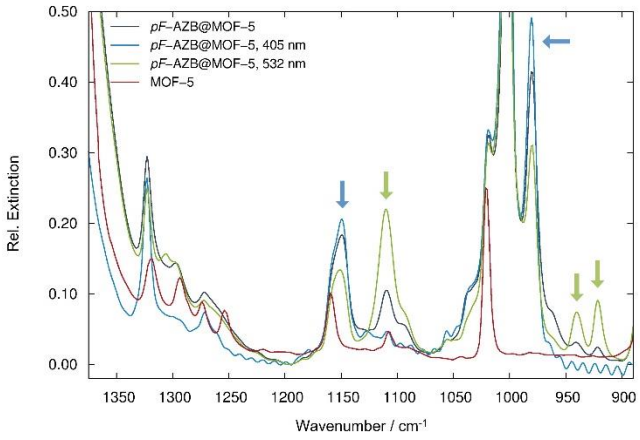

Figure 5. IR spectra of *pF*-AZB@MOF-5 after light induced isomerization with λ = 532 nm (*E*→*Z*) and λ = 405 nm (*Z*→*E*). The IR spectra of the ground state and pristine MOF-5 are given as a dark grey and a red curve, respectively. Arrows mark bands assigned to the *E* (blue) and *Z* (green) isomer.

We therefore used this approach to characterize the photochromic behavior of the novel guest@MOF systems. In Figure 5-7 and Figures S23-S25 (Supporting Information) the IR spectra we obtained before and after illumination with light of different wavelengths are given for *pF*-AZB@MOF-5, *tF*-AZB@MIL-68(In), and *pF*-AZB@MIL-68(In). After trying several wavelengths for photoswitching we observed that the optimal wavelengths were 532 nm for *E*→*Z* and 405 nm for *Z*→*E* switching. In Table 3 the results of the quantitative analyses of the IR spectra are summarized. For each of the investigated systems the maximum amounts of *E* and *Z* isomers are given, which were obtained in the illumination experiments. Additionally, the composition of the ground state (before illumination) is given. Details of the procedure, how we obtained these spectra and how we analyzed the *E*/*Z* ratio quantitatively, are given in the Experimental Section. In the following we will present a few selected examples to illustrate, how we investigated the photochromic behavior of the compounds under discussion.

According to the literature *E*-*pF*-AZB shows absorption maxima at λ = 310 nm and λ = 453 nm in solution.[52] We have chosen *pF*-$AZB_{3.57}$@MOF-5 for first illumination experiments with different wavelengths. The changes in the obtained IR spectra (Figure 5) after irradiation were compared with the spectra given in the literature and specific bands were assigned to the two isomers. For *pF*-$AZB_{3.57}$@MOF-5 the highest amount of *Z*-*pF*-AZB was obtained by illumination with green light (λ = 532 nm) in good agreement with the results obtained for solutions (cp. Table 1).[52] The back transformation *Z*→*E* was achieved by illumination with violet light (λ = 405 nm). Similarly, the isomerization of *tF*-AZB in solution was described with λ > 450 nm (*E*→*Z*, 91 %) and λ = 410 nm (*Z*→*E*, 86 %).[48,52] For *tF*-AZB embedded in MIL-68(In) (Figure 6) we achieved the highest amount of *E*→*Z* isomerization with λ = 532 nm and *Z*→*E* isomerization with λ = 405 nm, similar to *pF*-AZB. We also used λ = 476 nm to trigger the *E*→*Z* isomerization in *tF*-AZB@MIL-68(In). As can be seen in Figure 6 an *E*→*Z* isomerization is achieved, but the amount of the *Z* isomer is significantly smaller than the amount obtained with λ = 532 nm. With all other MOF hosts or with *oF*-AZB as third photochromic guest used in this investigation we achieved the best results (maximum of the respective photo isomer) by irradiation with λ = 532 nm (*E*→*Z*) and λ = 405 nm (*Z*→*E*). It is notable that like for solutions the fluorination of azobenzene allows photoswitching with visible light,[48,52] whereas for pristine azobenzene UV light (λ = 325 nm) has to be used for the *E*→*Z* isomerization.[40]

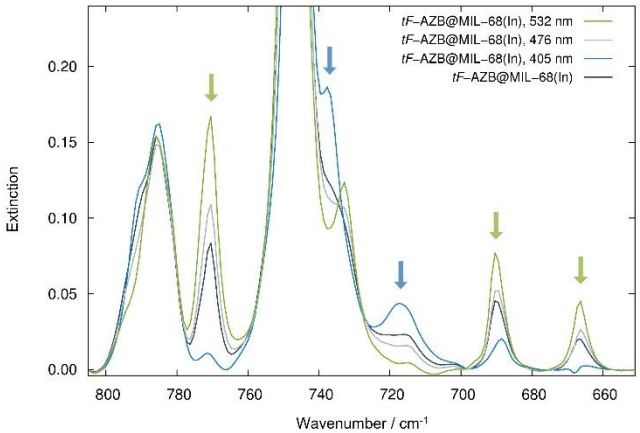

Figure 6. IR spectra of *tF*-AZB@MIL-68(In) after light induced isomerization with λ = 476 nm / 532 nm (*E*→*Z*) and λ = 405 nm (*Z*→*E*). The ground state is given as a dark grey curve. Arrows mark bands assigned to the *E* (blue) and *Z* (green) isomer.

It is remarkable that in some spectra the bands of one isomer are almost completely extinguished after irradiation. In *pF*-AZB@MIL-68(In) (Figure 7) the band at 1110 cm^{-1} that is assigned to *Z*-*pF*-AZB, is no longer observed after irradiation with violet light (λ = 405 nm), i.e. the *Z* isomer is completely transformed to the respective *E* isomer by irradiation. Similarly, the intensity of the band at approx. 770 cm^{-1} in *tF*-AZB@MIL-68(In) (Figure 6) decreases strongly upon irradiation with violet light, again pointing to an almost complete *Z*→*E* isomerization. Contrary, upon irradiation with green light (λ = 532 nm) the intensities of these bands increase strongly indicating a successful *E*→*Z* isomerization.

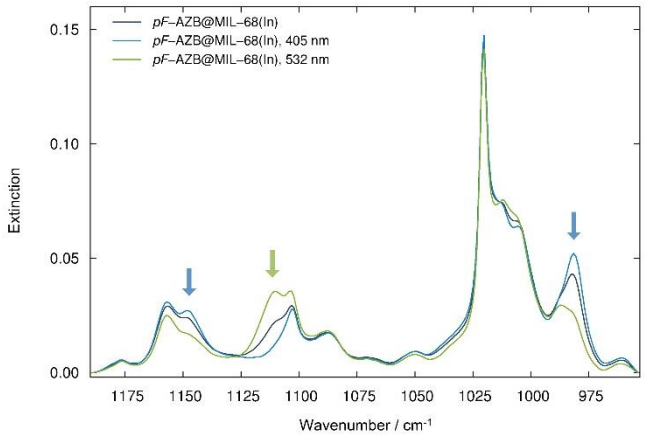

Figure 7. IR spectra of *pF*-AZB@MIL-68(In) after light induced isomerization with λ = 532 nm (*E*→*Z*) and λ = 405 nm (*Z*→*E*). The ground state is given as a dark grey curve. Arrows mark bands assigned to the *E* (blue) and *Z* (green) isomer.

In Table 3 the results of the quantitative analyses of the IR spectra are summarized. For each of the investigated systems the maximum amounts of *E* and *Z* isomers are given, which were obtained in the illumination experiments. Additionally, the composition of the ground state (before illumination) is given. As a reference pure crystalline *tF*-AZB was investigated under the same conditions (Figure S23a), Supporting Information). The ground state (before illumination) of *pF*-AZB consists of a mixture of both isomers and photochemical conversion of one isomer into the other was not possible in the crystalline material. In contrast, *tF*-AZB shows photo-isomerization in the solid state as well. By illumination of the ground state containing a mixture of both isomers with violet light (λ = 405 nm) a complete isomerization to 100 % *E*-*tF*-AZB was achieved. Illumination with green light (λ = 532 nm) led to 37 % of the *Z* isomer.

<Table 3>

As described in our former work[40] for AZB embedded in different MOF hosts only a maximum of 30 % *Z*-AZB was reached upon irradiation. For potential applications this is certainly a drawback like the need to use UV light for the photo-isomerization. As obvious from Table 3 the situation is different for fluorinated azobenzenes as photochromic guests embedded in different MOF hosts. All compounds with *pF*-AZB as guest molecule can be transferred to 100 % of the *E* isomer by illumination with violet light (λ = 405 nm). However, with green light only a maximum of 79 % *Z* isomer is achieved within a MIL-68(In) host. So for potential applications, hybrid materials with embedded *tF*-AZB seem to be preferable, as in almost all MOF hosts *E* and *Z* ratios above 90 % were reached (Table 3). One might speculate that the size of the MOF pores influences the photo-isomerization, as for *pF*-AZB as photochromic guest the largest *Z* ratio is observed within the large pores of MIL-68(In). However within the pores of MOF-5 with a similar size only 50 % of *Z*-*pF*-AZB were reached and no such size-dependence is observed for compounds with *tF*-AZB as guest. In Table 2 the shifts of OH frequencies of the MIL-53/MIL-68 frameworks upon guest loading are given. It is quite remarkable that upon irradiation and photo-isomerization these signals show the most significant shifts for systems with *tF*-AZB guests. Two exemplary IR spectra are given in Figure 8. This indicates that upon irradiation and photo-isomerization the host-guest and guest-guest interactions change in these *tF*-AZB@MOF systems. So the ratio of *E* and *Z* isomers seems to be less influenced by the pore size of the respective MOF host, but more siginficantly by the underlying host-guest and guest-guest interactions, which were discussed above for $AZB_{0.50}$@MIL-53(Al) and *pF*-$AZB_{0.34}$@MIL-53(Al) (Figure 4). For a rational design of an optimized guest@MOF system it seems to be essential to understand these interactions in more detail.

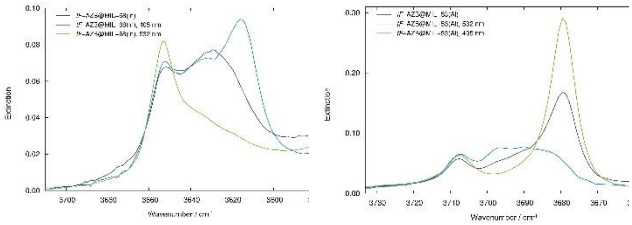

Figure 8. Sections (regime of OH frequencies) of the IR spectra of *tF*-AZB@MIL-68(In) (left) and *tF*-AZB@MIL-53(Al) (right) after light induced isomerization with λ = 532 nm (*E*→*Z*) and λ = 405 nm (*Z*→*E*). The ground state is given as a dark grey curve.

It was a remarkable finding of our work on AZB embedded in different MOFs that for $AZB_{0.50}$@MIL-53(Al) no photo-isomerization was achieved even after very long irradiation times.[40] From the crystal structure it was concluded that the AZB guests are densely packed within the pores of MIL-53(Al) so that photo-isomerization is hindered for sterical reasons.[40] As can be seen in Table 3, *tF*-AZB (100 % *Z*), *oF*-AZB (56 % *Z*), and *pF*-AZB ("little *Z*") embedded in MIL-53(Al) allow photo-isomerization, at least to some extent. But from chemical analysis (Table S4, Supporting Information) it was found that the loading in this systems is different: $guest_x$@MIL-53(Al) with x = 0.50 for AZB, x = 0.19 for *tF*-AZB, x = 0.18 for *oF*-AZB, and x = 0.30 (or 0.34 depending on the analytical method) for *pF*-AZB. Even when considering the different volumes of the guests (AZB: V/Z = 248.33(5) Å^3; *tF*-AZB: V/Z = 272.90(2) Å^3; *oF*-AZB: V/Z = 289.90(5) Å^3; *pF*-AZB: V/Z = 284.65(5) Å^3)[50] the packing of AZB (x = 0.50) within the pores of MIL-53(Al) is much denser than that of *tF*-AZB (x = 0.19) so that the different Z ratios from 0 % to 100 % are not surprising.

Kitagawa and co-workers embedded AZB in flexible DMOF-1 and found that the photo-isomerization of the AZB guest triggered a reversible structural transformation of the MOF framework, which was used to remote-control the uptake and release of CO_2.[39] This structural transformation was reached, although photo-isomerization only

led to a *Z*/*E* ratio of 38:62.[39] As MIL-53(Al) and its Ga analogue are also known to show flexible ("breathing") behavior upon guest inclusion,[54,55] we tested our guest@MIL-53 systems for such behavior. In Figures S26 and S27 (Supporting Information) the synchrotron powder diffraction patterns of *tF*-$AZB_{0.19}$@MIL-53(Al) (capillary, ∅ = 0.3 mm) after irradiation with green (λ = 532 nm; several hours) and violet light (λ = 405 nm; several hours) are compared with those of non-irradiated *tF*-$AZB_{0.19}$@MIL-53(Al). As the reflection positions are unchanged no structural transformation has taken place under these conditions. Slight changes of the reflection intensities indicate a different arrangement of the *tF*-AZB guests within the pores of MIL-53(Al). In Figure S28 (Supporting Information) smaller sections of the synchrotron powder diffraction patterns are compared. The reflections obtained upon violet light irradiation (λ = 405 nm, *Z*→*E* isomerization) appear slightly broadened. The reasons for this are unknown at the moment. Comparing the lattice parameters of MIL-53(Al) with different guests (Table S2, Supporting Information) an increase of 3.1 % from 1399.66 Å³ ($AZB_{0.50}$@MIL-53(Al)) to 1444.0 Å³ (*pF*-$AZB_{0.34}$@MIL-53(Al)) is observed. This increase seems to be significant and might be a result of the different host-guest and guest-guest interactions in these compounds, but the value is far smaller than the typical volume decreases found for breathing MIL-53(Al) (approx. 33 %).[54] It should be noted that also the low penetration depth of UV/vis light into solid matter might be the reason for the observation that no structural changes of MIL-53(Al) were observed, although we already used a capillary with a small diameter of only 0.3 mm. Notably, differing results were published for structural transformations of flexible MOF hosts induced by photo-isomerization of embedded guests. *Kitagawa* and co-workers reported such an effect for AZB embedded in flexible DMOF-1,[39] whereas photo-isomerization of related PAP (2-phenylazopyridine)[74] or DTE (1,2-bis(2,5-dimethyl-thien-3-yl)-perfluorocyclopentene)[43] did not lead to a structural transformation of the same host upon irradiation.

CONCLUSION

In summary, we have synthesized and characterized 15 new photochromic materials by embedment of fluorinated azobenzenes, namely *ortho*-tetrafluoroazobenzene (*tF*-AZB), 4H,4H'-octafluoroazobenzene (*oF*-AZB), and perfluoroazobenzene (*pF*-AZB), into the pores of the five well-known MOFs, i.e. MOF-5, MIL-53(Al), MIL-53(Ga), MIL-68(Ga), and MIL-68(In). The successful embedment was confirmed by X-ray powder diffraction and the amount of loading determined from elemental (CHNS), DSC/TGA, and – for one example – Rietveld analysis. The latter was performed on *pF*-$AZB_{0.34}$@MIL-53(Al). From the resulting crystal structure host-guest and guest-guest interactions were elucidated revealing O-H···F and π···π type interactions, which were compared with the interactions found in the already described crystal structure of $AZB_{0.5}$@MIL-53(Al). In compounds with MOFs of the MIL-type series shifts of the O-H frequencies of the respective hosts were used to quantitatively assign these interactions. Notably, the largest shifts and thus strongest interactions were found for unfluorinated azobenzene as guest. Similarly, Bléger and co-workers used the O-H stretching frequencies of an UiO-66 type MOF with *tF*-AZB side groups to follow the photo-isomerization in this system.[35]

But the most remarkable finding of these investigations is that for some of the synthesized *F*-AZB@MOF systems an almost quantitative (> 95 %) switching between *E* and *Z* isomers was observed in a solid state material. Quantitative switching in solids is still rare, but not unprecedented.[36,76] From the results of the photophysical investigations summarized in Table 3 *tF*-AZB seems to be the most interesting guest molecule, which already showed very remarkable photochromic properties in solution (Table 1) or as a side group in other MOFs.[35,36] With respect to the host MIL-68(In) seems to be preferable due to its higher chemical stability compared to e.g. MOF-5 and the high photo-isomerization rates that were achieved with this host (Table 3). Therefore we have chosen *tF*-$AZB_{0.57}$@MIL-68(In) to investigate the photochemical stability of this system. In Figure 9 the ratio of *E*-*tF*-AZB after three switching cycles with λ = 532 nm and λ = 405 nm, resp. is shown, which reveal no significant fatigue in these measurements. For possible applications it should be noted that a successful synthesis of thin films of MIL-68(In) has already been described.[75]

To improve the photochromic properties of the presented *F*-AZB@MOF systems it seems to be essential to understand the underlying host-guest and guest-guest interactions in more detail. In our investigation we give first insights how these interactions can be determined. It is very remarkable that for *tF*-AZB as guest the IR frequencies show the most significant shifts upon photo-isomerization (Table 2). This indicates that the host-guest and guest-guest interactions change upon *E*/*Z* isomerization so that influencing these interactions might help to improve the photochromic properties of these compounds. We found that the photochromic properties are also affected by the size/shape of the MOF's pore as well as the degree of guest loading, i.e. the packing of the guest molecules within the MOF's pores. With respect to the chemical environment within the pores we found earlier that the nature of the metal / metal-oxo knot also influences the photochromic properties,[42] whereas the influence of the linker ligand still needs to be explored. All these considerations lead to the conclusion that host-guest and guest-guest interactions in these guest@MOF materials need to be investigated in much more detail.

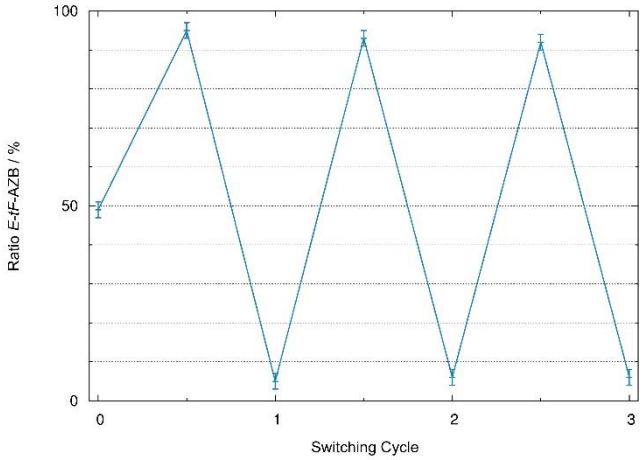

Figure 9. Ratio of *E*-*tF*-AZB in *tF*-$AZB_{0.57}$@MIL-68(In) after three switching cycles and irradiation with λ = 532 nm and λ = 405 nm, resp.. For the standard deviation a value of ± 2 % was estimated.

ASSOCIATED CONTENT

The Supporting Information is available free of charge on the ACS Publications website at DOI: ...
Details of synthesis, elemental analyses, photographs of resulting materials, XRPD patterns of loaded and unloaded MOFs (Le Bail and Rietveld fits), IR spectra and XRPD patterns before and after illumination with light, DSC/TGA curves (PDF)

AUTHOR INFORMATION

Corresponding Author

*E-mail for U.R.: Uwe.Ruschewitz@uni-koeln.de.

ORCID

Uwe Ruschewitz: 0000-0002-6511-6894

Dominik Schaniel: 0000-0003-2440-9540

Heidi A. Schwartz: 0000-0001-9894-1527

Author Contributions

D.H. performed the syntheses and all experiments, which were coplanned by D.H. and U.R.. D.S. provided the different spectroscopic instruments as well as his expertise in performing and analyzing the data obtained with these methods. H.A.S. and M.W. added the TGA/DSC analyses. All authors discussed the results and the final version of the manuscript, which was written by D.H. and U.R..

Funding Sources

D.H. acknowledges the Fonds der Chemischen Industrie for a doctoral stipend.

Notes

The authors declare no competing financial interest.

ACKNOWLEDGMENT

The authors gratefully acknowledge H. Emerich and C. Sternemann for their technical support and expertise at BM01B (ESRF/Grenoble) and BL9 (DELTA/Dortmund), S. Kremer for the elemental analyses, M. Prechtl for providing his IR spectrometer housed in a glovebox, and BASF SE for donating MOF-5.

REFERENCES

(1) Bouas-Laurent, H.; Dürr, H. Organic Photochromism. *Pure Appl. Chem.* **2001**, *73*, 639-665.
(2) Parthenopoulos, D. A.; Renetzepis, P. M. Three-dimensional optical storage memory. *Science* **1989**, *245*, 843-845.
(3) Hirshberg, Y. Photochromie Dans Le Série de La Bianthrone. *C. R. Hebd. Seánces Acad. Sci.* **1950**, *116*, 903–904.
(4) Li, C.; Zhang, Y.; Hu, J.; Cheng, J.; Liu, S. Reversible Three-State Switching of Multicolor Fluorescence Emission by Multiple Stimuli Modulated FRET Processes within Thermoresponsive Polymeric Micelles. *Angew. Chem. Int. Ed.* **2010**, *49*, 5120-5124.
(5) Liao, B.; Long, P.; He, B.; Yi, S.; Ou, B.; Shen, S.; Chen, J. Reversible fluorescence modulation of spiropyran-functionalized carbon nanoparticles. *J. Mater. Chem. C* **2013**, *1*, 3716-3721.
(6) Chen, J.; Zeng, F.; Wu, S.; Zhao, J.; Chen, Q.; Tong, Z. Reversible fluorescence modulation through energy transfer with ABC triblock copolymer micelles as scaffolds. *Chem. Commun.* **2008**, *13*, 5580-5582.
(7) Zhu, L.; Zhu, M.-Q.; Hurst, J. K.; Li, A. D. Q. Light-Controlled Molecular Switches Modulate Nanocrystal Fluorescence. *J. Am. Chem. Soc.* **2005**, *127*, 8968-8970.
(8) Bléger, D.; Dokić, J.; Peters, M. V.; Grubert, L.; Saalfrank, P.; Hecht, S. Electronic Decoupling Approach to Quantitative Photoswitching in Linear Multiazobenzene Architectures. *J. Phys. Chem. B.* **2011**, *115*, 9930-9940.
(9) Chung, D.-J.; Ito, Y.; Imanishi, Y. Preparation of porous membranes grafted with poly(spiropyran-containing methacrylate) and photocontrol of permeability. *J. Appl. Polym. Sci.* **1994**, *51*, 2027–2033.
(10) Moniruzzaman, M.; Sabey C. J.; Fernando, G. F. Photoresponsive polymers: An investigation of their photoinduced temperature changes during photoviscosity measurements. *Polymer* **2007**, *48*, 255–263.
(11) Bléger, D.; Liebig, T.; Thiermann, R.; Maskos, M.; Rabe, J. P.; Hecht, S. Light-Orchestrated Macromolecular "Accordions": Reversible Photoinduced Shrinking of Rigid-Rod Polymers. *Angew. Chem. Int. Ed.* **2011**, *50*, 12559-12563.
(12) Alemani, M.; Selvanathan, S.; Ample, F.; Peters, M. V.; Rieder, K.-H.; Moresco, F.; Joachim, C.; Hecht, S.; Grill, L. Adsorption and Switching Properties of Azobenzene Derivatives on Different Noble Metal Surfaces: Au(111), Cu(111), and Au(100). *J. Phys. Chem. C* **2008**, *112*, 10509-10514.
(13) Klajn, R. Spiropyran-based dynamic materials. *Chem. Soc. Rev.* **2014**, *43*, 148–184.
(14) Tomioka, H.; Itoh, T. Photochromism of Spiropyrans in Organized Molecular Assemblies. Formation of J- and H-Aggregates of Photomerocyanines in Bilayers-Clay Matrices. *Chem. Commun.* **1991**, *7*, 532–533.
(15) Irie, M.; Fukaminato, T.; Matsuda, K.; Kobatake, S. Photochromism of Diarylethene Molecules and Crystals: Memories, Switches, and Actuators. *Chem. Rev.* **2014**, *114*, 12174-12277.
(16) Marlow, F.; Hoffmann, K.; Caro, J. Photoinduced switching in nanocomposites of azobenzene and molecular sieves. *Adv. Mater.* **1997**, *9*, 567–570.
(17) Weh, K.; Noack, M.; Hoffmann, K.; Schröder, K.-P.; Caro, J.; Change of gas permeation by photoinduced switching

of zeolite azobenzene membranes of type MFI and FAU. *Microporous Mesoporous Mater.* **2002**, *54*, 15–26.
(18) Hoffmann, K.; Resch-Genger, U.; Marlow, F. Photoinduced switching of nanocomposites consisting of azobenzene and molecular sieves: investigation of the switching states. *Microporous Mesoporous Mater.* **2000**, *41*, 99–106.
(19) Qu, D.-H.; Wang, Q.-C.; Zhang, Q.-W.; Ma, X., Tian, H. Photoresponsive Host–Guest Functional Systems. *Chem. Rev.* **2015**, *115*, 7543-7588.
(20) Samanta, D.; Gemen, J.; Chu, Z.; Diskin-Posner, Y.; Shimon, L. J. W.; Klajn, R. Reversible photoswitching of encapsulated azobenzenes in water. *Proc. Natl. Acad. Sci. USA* **2018**, https://doi.org/10.1073/pnas.1712787115.
(21) Castellanos, S.; Kapteijn, F.; Gascon, J. Photoswitchable Metal Organic Frameworks: Turn on the Lights and Close the Windows. *CrystEngComm* **2016**, *18*, 4006–4012.
(22) Wang, L.; Li, Q. Photochromism into nanosystems: towards lighting up the future nanoworld. *Chem. Soc. Rev.* **2018**, *47*, 1044-1097.
(23) Dolgopolova, E. A.; Rice, A. M.; Martin, C. R.; Shustova, N. B. Photochemistry and photophysics of MOFs: steps towards MOF-based sensing enhancements. *Chem. Soc. Rev.* **2018**, *47*, 4710-4728.
(24) Férey, G. Hybrid porous solids: past, present, future. *Chem. Soc. Rev.* **2008**, *37*, 191-214.
(25) Janiak, C. Engineering coordination polymers towards applications. *Dalton Trans.* **2003**, 2781-2804.
(26) Schaate, A.; Dühnen, S.; Platz, G.; Lilienthal, S.; Schneider, A. M.; Behrens, P. A Novel Zr-Based Porous Coordination Polymer Containing Azobenzenedicarboxylate as a Linker. *Eur. J. Inorg. Chem.* **2012**, 790–796.
(27) Epley, C. C.; Roth, K. L.; Lin, S.; Ahrenholtz, S. R.; Grove, T. Z.; Morris, A. J. Cargo delivery on demand from photodegradable MOF nano-cages. *Dalton Trans.* **2017**, *46*, 4917–4922.
(28) Zhang, J.; Wang, L.; Li, N.; Liu, J.; Zhang, W.; Zhang, Z.; Zhou, N.; Zhu, X. A novel azobenzene covalent organic framework. *CrystEngComm* **2014**, *16*, 6547–6551.
(29) Modrow, A.; Zargarani, D.; Herges, R.; Stock, N. The first porous MOF with photoswitchable linker molecule. *Dalton Trans.* **2011**, *40*, 4217-4222.
(30) Park, J.; Yuan, D.; Pham, K. T.; Li, J.-R.; Yakovenko, A.; Zhou, H.-C. Reversible alteration of CO_2 adsorption upon photochemical or thermal treatment in a metal-organic framework. *J. Am. Chem. Soc.* **2012**, *134*, 99–102.
(31) Yu, X.; Wang, Z.; Buchholz, M.; Füllgrabe, N.; Grosjean, S.; Bebensee, F.; Bräse, S.; Wöll, C.; Heinke, L. *cis*-to-*trans* isomerization of azobenzene investigated by using thin films of metal–organic frameworks. *Phys. Chem. Chem. Phys.* **2015**, *17*, 22721–22725.
(32) Heinke, L.; Cakici, M.; Dommaschk, M.; Grosjean, S.; Herges, R.; Bräse, S.; Wöll, C. Photoswitching in two-component surface-mounted metal-organic frameworks: optically triggered release from a molecular container. *ACS Nano* **2014**, *8*, 1463–1467.
(33) Heinke, L. Diffusion and photoswitching in nanoporous thin films of metal-organic frameworks. *J. Phys. D. Appl. Phys.* **2017**, *50*, 193004.
(34) Kanj, A. B.; Müller, K.; Heinke, L. Stimuli-Responsive Metal-Organic Frameworks with Photoswitchable Azobenzene Side Groups. *Macromol. Rapid Commun.* **2018**, *39*, 1700239 (14 pages).
(35) Castellanos, S.; Goulet-Hanssens, A.; Zhao, F.; Dikhtiarenko, A.; Pustovarenko, A.; Hecht, S.; Gascon, J.; Kapteijn, F.; Bléger, D. Structural Effects in Visible-Light-Responsive Metal–Organic Frameworks Incorporating ortho-Fluoroazobenzenes. *Chem. Eur. J.* **2016**, *22*, 746-752.
(36) Müller, K.; Knebel, A.; Zhao, F.; Bléger, D.; Caro, J.; Heinke, L. Switching Thin Films of Azobenzene-Containing Metal–Organic Frameworks with Visible Light. *Chem. Eur. J.* **2017**, *23*, 5434-5438.
(37) Williams, D. E.; Martin, C. R.; Dolgopolova, E. A.; Swifton, A.; Godfrey, D. C.; Ejegbavwo, O. A.; Pellechia, P. J.; Smith, M. D.; Shustova, N. B. Flipping the Switch: Fast Photoisomerization in a Confined Environment. *J. Am. Chem. Soc.* **2018**, *140*, 7611-7622.
(38) Schwartz, H. A.; Ruschewitz, U.; Heinke, L. Smart Nanoporous Metal-Organic Frameworks by Embedding Photochromic Molecules – State of the Art and Future Perspectives. *Photochem. Photobiol. Sci.* **2018**, *17*, 864-873.
(39) Yanai, N.; Uemura, T.; Inoue, M.; Matsuda, R.; Fukushima, T.; Tsujimoto, M.; Isoda, S.; Kitagawa, S. Guest-to-host transmission of structural changes for stimuli-responsive adsorption property. *J. Am. Chem. Soc.* **2012**, *134*, 4501–4504.
(40) Hermann, D.; Emerich, H.; Lepski, R.; Schaniel, D.; Ruschewitz, U. Metal–Organic Frameworks as Hosts for Photochromic Guest Molecules. *Inorg. Chem.* **2013**, *52*, 2744–2749.
(41) Zhang, F.; Zou, X.; Feng, W.; Zhao, X.; Jing, X.; Sun, F.; Ren, H.; Zhu, G. Microwave-assisted crystallization inclusion of spiropyran molecules in indium trimesate films with antidromic reversible photochromism. *J. Mater. Chem.* **2012**, *22*, 25019–25026.
(42) Schwartz, H. A.; Olthof, S.; Schaniel, D.; Meerholz, K.; Ruschewitz, U. Solution-Like Behavior of Photoswitchable Spiropyrans Embedded in Metal–Organic Frameworks. *Inorg. Chem.* **2017**, *56*, 13100–13110.
(43) Walton, I. M.; Cox, J. M.; Coppin, J. A.; Linderman, C. M.; Patel, D. G.; Benedict, J. B. Photo-responsive MOFs: light-induced switching of porous single crystals containing a photochromic diarylethene. *Chem. Commun.* **2013**, *49*, 8012–8014.
(44) Ohara, K.; Inokuma, Y.; Fujita, M. The catalytic *Z* to *E* isomerization of stilbenes in a photosensitizing porous coordination network. *Angew. Chem. Int. Ed.* **2010**, *49*, 5507-5509.
(45) Zheng, Y.; Sato, H.; Wu, P.; Jeon, H. J.; Matsuda, R.; Kitagawa, S. Flexible interlocked porous frameworks allow quantitative photoisomerization in a crystalline solid. *Nat. Commun.* **2017**, *8*, Article number: 100.
(46) Kojima, M.; Nakajoh, M.; Nebashi, S.; Kurita, N. Effect of metal cation on photoisomerization of azobenzenes in zeolite nanocavities. *Res. Chem. Intermed.* **2004**, *30*, 181-190.
(47) Wegner, H. A. Azobenzenes in a new light-switching in vivo. *Angew. Chem. Int. Ed.* **2012**, *51*, 4787–4788.
(48) Bléger, D.; Schwarz, J.; Brouwer, A. M.; Hecht, S. *o*-Fluoroazobenzenes as Readily Synthesized Photoswitches Offering Nearly Quantitative Two-Way Isomerization with Visible Light. *J. Am. Chem. Soc.* **2012**, *134*, 20597–20600.
(49) Müller, K.; Wadhwa, J.; Malhi, J. S.; Schöttner, L.; Welle, A.; Schwartz, H.; Hermann, D.; Ruschewitz, U.; Heinke, L. Photoswitchable nanoporous films by loading azobenzene in metal–organic frameworks of type HKUST-1. *Chem. Commun.* **2017**, *53*, 8070-8073.
(50) Hermann, D.; Schwartz, H. A.; Ruschewitz, U. Crystal Structures of *Z* and *E ortho*-Tetrafluoroazobenzene. *ChemistrySelect* **2017**, *2*, 11846–11852.
(51) Bandara, H. M. D.; Burdette, S. C. Photoisomerization in different classes of azobenzene. *Chem. Soc. Rev.* **2012**, *41*, 1809-1825.
(52) Knie,C.; Utecht, M.; Zhao, F.; Kulla, H.; Kovalenko, S.;

Brouwer, A. M.; Saalfrank, P.; Hecht, S.; Bléger, D. *ortho*-Fluoroazobenzenes: Visible Light Switches with Very Long-Lived *Z* Isomers. *Chem. Eur. J.* **2014**, *20*, 16492–16501.
(53) Li, H.; Eddaoudi, M.; O'Keeffe, M.; Yaghi, O. M. Design and synthesis of an exceptionally stable and highly porous metal-organic framework. *Nature* **1999**, *402*, 276-279.
(54) Loiseau, T.; Serre, C.; Huguenard, C.; Fink, G.; Taulelle, F.; Henry, M.; Bataille, T.; Férey, G. A rationale for the large breathing of the porous aluminum terephthalate (MIL-53) upon hydration. *Chem. Eur. J.* **2004**, *10*, 1373-1382.
(55) Volkringer, C.; Loiseau, T.; Guillou, N.; Férey, G.; Elkaïm, E.; Vimont, A. XRD and IR structural investigations of a particular breathing effect in the MOF-type gallium terephthalate MIL-53(Ga). *Dalton Trans.* **2009**, 2241-2249.
(56) Volkringer, C.; Meddouri, M.; Loiseau, T.; Guillou, N.; Marrot, J.; Férey, G.; Haouas, M.; Taulelle, F.; Audebrand, N.; Latroche, M. The Kagomé topology of the gallium and indium metal-organic framework types with a MIL-68 structure: synthesis, XRD, solid-state NMR characterizations, and hydrogen adsorption. *Inorg. Chem.* **2008**, *47*, 11892-11901.
(57) Birchall, J. M.; Haszeldine, R. N.; Kemp, J. E. G. Polyfluoroarenes. Part X. Polyfluoroaromatic azo-compounds. *J. Chem. Soc. C* **1970**, 449-455.
(58) Hettel, S. PhD thesis, University of Cologne (Germany), **2009**.
(59) Van Beek, W.; Safonova, O. V.; Wiker, G.; Emerich, H. SNBL, a dedicated beamline for combined *in situ* X-ray diffraction, X-ray absorption and Raman scattering experiments. *Phase Transitions* **2011**, *84*, 726–732.
(60) Krywka, C.; Sternemann, C.; Paulus, M.; Javid, N.; Winter, R.; Al-Sawalmih, A.; Yi, S.; Raabe, D.; Tolan, M. The small-angle and wide-angle X-ray scattering set-up at beamline BL9 of DELTA. *J. Synchrotron Radiat.* **2007**, *14*, 244–251.
(61) *STOE Win XPOW 1.07*, STOE & Cie GmbH, Darmstadt, Germany, **2000**.
(62) Petríček, V.; Dušek, M.; Palatinus, L. Jana2006: The Crystallographic Computing System; Institute of Physics, Praha, Czech Republic, **2006**.
(63) Williams, T.; Kelley, C.; Lang, R. *Gnuplot 4.6*, **2012**.
(64) Vougo-Zanda, M.; Huang, J.; Anokhina, E.; Wang, X.; Jacobson, A. J. Tossing and turning: guests in the flexible frameworks of metal(III) dicarboxylates. *Inorg. Chem.* **2008**, *47*, 11535-11542.
(65) Chinnakali, K.; Fun, H.-K. Structure of *trans*-decafluoroazobenzene. *Acta Crystallogr.* **1993**, *C49*, 615-616.
(66) Favre-Nicolin, V.; Černý, R. *FOX*, `free objects for crystallography': a modular approach to *ab initio* structure determination from powder diffraction. *J. Appl. Crystallogr.* **2002**, *35*, 734-743.
(67) a) Larson, A. C.; v. Dreele, R. B. General Structure Analysis System (GSAS). *Los Alamos National Laboratory Report LAUR* **2004**, 86-748; b) Toby, B. H. EXPGUI, a graphical user interface for GSAS. *J. Appl. Crystallogr.* **2001**, *34*, 210–213.
(68) Brandenburg, K. *Diamond 3.2i*, Crystal Impact GbR, Bonn, Germany, **2012**.
(69) ACD/NMR Processor Academic Edition 12.01, Advanced Chemistry Development, Inc., **2010**.
(70) *OriginPro* Version 8.5.0G, OriginLab Corporation, Northhampton USA, **1991–2010**.
(71) Rowland, R. S.; Taylor, R. Intermolecular Nonbonded Contact Distances in Organic Crystal Structures: Comparison with Distances Expected from van der Waals Radii. *J. Phys. Chem.* **1996**, *100*, 7384-7391.
(72) Hernández-Trujillo, J.; Vela, A. Molecular Quadrupole Moments for the Series of Fluoro- and Chlorobenzenes. *J. Phys. Chem.* **1996**, *100*, 6524–6530.
(73) Hunter, C. A.; Lawson, K. R.; Perkins, J.; Urch, C. J. Aromatic interactions. *J. Chem. Soc., Perkin Trans.* **2001**, *2*, 651–669.
(74) Das, D.; Agarkar, H. Unexpected Nonresponsive Behavior of a Flexible Metal-Organic Framework under Conformational Changes of a Photoresponsive Guest Molecule *ACS Omega* **2018**, *3*, 7630-7638.
(75) Liu, J.; Zhang, F.; Zou, X.; Zhou, S.; Li, L.; Sun, F.; Qiu, S. Facile Synthesis of MIL-68(In) Films with Controllable Morphology. *Eur. J. Inorg. Chem.* **2012**, 5784-5790.
(76) Kobatake, S.; Takami, S.; Muto, H.; Ishikawa, T.; Irie, M. Rapid and reversible shape changes of molecular crystals on photoirradiation. *Nature* **2007**, *446*, 778–781.

Table 1. Selected optical properties of different azobenzenes.

	absorption maxima	photoisomerization	thermal half-life of *Z* isomer	Reference(s)
E-AZB	320 nm (π,π*) 450 nm (n,π*)	46-53 % *Z*-AZB (λ = 366 nm, cyclohexane)	$t_{1/2}$ = 2 days (room temperature) $t_{1/2}$ = 4 h (60 °C, acetonitrile)	[46,51,52]
Z-AZB	250, 270 nm (π,π*) 450 nm (n,π*)			
E-*tF*-AZB	305 nm (π,π*) 458 nm (n,π*)	84 % *Z*-*tF*-AZB (λ = 313 nm, acetonitrile) 91 % *Z*-*tF*-AZB (λ > 450 nm, acetonitrile)	$t_{1/2}$ = 700 days (25 °C) $t_{1/2}$ = 92 h (60 °C)	[48,52]
Z-*tF*-AZB	414 nm (n,π*)	86 % *E*-*tF*-AZB (λ = 410 nm, acetonitrile)		
E-*oF*-AZB	303 nm (π,π*) 456 nm (n,π*)	92 % *Z*-*oF*-AZB (λ > 500 nm, acetonitrile)	$t_{1/2}$ = 27 h (60 °C)	[52]
Z-*oF*-AZB	~240 nm (π,π*) 413 nm (n,π*)	92 % *E*-*oF*-AZB (λ = 410 nm, acetonitrile)		
E-*pF*-AZB	310 nm (π,π*) 453 nm (n,π*)	91 % *Z*-*pF*-AZB (λ > 500 nm, acetonitrile)	not determined	[52]
Z-*pF*-AZB	413 nm (n,π*)	90 % *E*-*pF*-AZB (λ = 410 nm, acetonitrile)		

Table 3. Maximum amounts of *E* and *Z* isomers for the investigated *F*-AZB@MOF systems, achieved by illumination with 405 and 532 nm, respectively.

	AZB[40] max. *E* / max. *Z* [ground state]	*tF*-AZB max. *E* / max. *Z* [ground state]	*oF*-AZB max. *E* / max. *Z* [ground state]	*pF*-AZB max. *E* / max. *Z* [ground state]
MOF-5	100 % / 25 % [100 % *E*]	93 % / 82 % [52 % *E*]	n.d. [62–88 % *E*]	100 % / 50 % [80 % *E*]
MIL-53(Al)	100 % / 0 % [100 % *E*]	90 % / 100 % [37 % *E*]	100 % / 56 % [99 % *E*]	100 % / little *Z* [100 % *E*]
MIL-53(Ga)	100 % / n.d. [100 % *E*]	90 % / 94 % [37 % *E*]	n.d. [little *Z*]	100 % / n.d. [100 % *E*]
MIL-68(Ga)	100 % / 27 % [100 % *E*]	96 % / 93 % [45 % *E*]	n.d. [62–88 % *E*]	100 % / 40 % [87 % *E*]
MIL-68(In)	100 % / 30 % [100 % *E*]	95 % / 95 % [51 % *E*]	88 % / 90 % [62 % *E*]	100 % / 79 % [55 % *E*]

* n.d.: not determined

Insert Table of Contents artwork here